Clinical Cancer Research

# Pharmacologic Inhibition of JAK1/JAK2 Signaling Reduces Experimental Murine Acute GVHD While Preserving GVT Effects

Cristiana Carniti[1], Silvia Gimondi[1], Antonio Vendramin[1], Camilla Recordati[2], Davide Confalonieri[1], Anisa Bermema[1], Paolo Corradini[1,3], and Jacopo Mariotti[1]

## Abstract

**Purpose:** Immune-mediated graft-versus-tumor (GVT) effects can occur after allogeneic hematopoietic stem cell transplantation (HSCT), but GVT is tightly linked to its main complication, graft-versus-host disease (GVHD). Strategies aimed at modulating GVHD, while maintaining the GVT effect, are needed to improve the cure rate of transplant. Given the emerging role of Janus-activated kinase (JAK) signaling in lymphoproliferative and myeloproliferative diseases and its established function at dictating T-cell differentiation, we postulated that JAKs might be potential therapeutic targets through a pharmacologic approach.

**Experimental Design:** We examined the effect of JAK1/JAK2 modulation by ruxolitinib in a mouse model of fully MHC mismatched bone marrow transplant comprising *in vivo* tumor inoculation.

**Results:** JAK1/JAK2 inhibition by ruxolitinib improved both overall survival ($P = 0.03$) and acute GVHD pathologic score at target organs ($P \leq 0.001$) of treated mice. In addition, treatment with ruxolitinib was associated with a preserved GVT effect, as evidenced by reduction of tumor burden ($P = 0.001$) and increase of survival time ($P = 0.01$). JAK1/JAK2 inhibition did not impair the *in vivo* acquisition of donor T-cell alloreactivity; this observation may account, at least in part, to the preserved GVT effect. Rather, JAK1/JAK2 inhibition of GVHD was associated with the modulation of chemokine receptor expression, which may have been one factor in the reduced infiltration of donor T cells in GVHD target organs.

**Conclusions:** These data provide further evidence that JAK inhibition represents a new and potentially clinically relevant approach to GVHD prevention. *Clin Cancer Res; 21(16); 3740–9.* ©2015 AACR.

## Introduction

Allogeneic hematopoietic stem cell transplantation (HSCT) represents a potential curative strategy for patients with several hematologic malignancies (1). Donor immune system mediates the beneficial graft-versus-tumor (GVT) effect, but can also result in acute graft-versus-host disease (GVHD) that, despite recent improvements in the transplantation procedure and supportive care (2), remains a major contributor to transplantation-related deaths and the most significant barrier to the success of allogeneic-HSCT (3). In general, attempts to prevent GVHD are often associated with a reduction in GVT effects. Therefore, approaches aimed at separating GVT effect from GVHD are warranted, but are difficult to achieve because of their shared biology (4). Different strategies have been proposed in preclinical mouse models of acute GVHD, including those targeting NK activation, DC maturation, or T cell response, such as T-cell activation, signaling pathway, and homing to GVHD target organs (5). Of note, preserving the GVT effect was not always a prerequisite of these studies. More recently, blockade of visceral lymphocyte chemotaxis resulted in reduced incidence of clinical acute GVHD (6).

The Janus-activated kinases (JAK) family forms one subgroup of nonreceptor protein kinases that are involved in cell growth, survival, and differentiation of various cell populations, mainly through the activation of "signal transducers and activators of transcription" proteins (STATs). JAK2 signaling was shown to be of relevance for the pathogenesis myeloid and lymphoid malignancies (7, 8) and similarly an aberrant activation of the JAK–STAT pathway was linked to the oncogenic process and outcome of Hodgkin and non-Hodgkin lymphomas (9–11). Moreover, a significant improvement for the treatment of patients with myelofibrosis was recently achieved by the introduction of the JAK1/JAK2-specific inhibitor, ruxolitinib (12). Another fundamental role of JAK–STAT signaling is to dictate immune cells activation and differentiation (13). We have previously shown that STAT signaling is not dispensable for development of T-cell alloreactivity (14) in graft rejection experiments and that STAT3 activation is of fundamental importance for the onset of acute GVHD (15). In addition, other reports have extensively studied the role of different proteins of the STATs family for the onset of GVHD (16, 17). More recently, *in vitro* JAK2 inhibition resulted in reduced activation of dendritic cells (DC) and induced durable tolerance to alloantigen of T cells primed by ruxolitinib-modified DCs (18).

[1]Department of Hematology, Fondazione IRCCS Istituto Nazionale dei Tumori, Milan, Italy. [2]Mouse and Animal Pathology Laboratory, Fondazione Filarete, Milan, Italy. [3]Chair of Hematology, Università degli Studi di Milano, Milan, Italy.

**Note:** Supplementary data for this article are available at Clinical Cancer Research Online (http://clincancerres.aacrjournals.org/).

P. Corradini and J. Mariotti contributed equally to this article and share last authorship.

**Corresponding Author:** Jacopo Mariotti, Department of Hematology, Fondazione IRCCS Istituto Nazionale dei Tumori, via Venezian 1, 20133, Milan, Italy. Phone: 39-0223902917; Fax: 39-0223902908; E-mail: jacopo.mariotti@istitutotumori.mi.it

**doi:** 10.1158/1078-0432.CCR-14-2758





AACR

## Translational Relevance

Hematopoietic stem cell transplantation is a commonly used immunotherapy method, but its curative potential, the so-called graft-versus-tumor (GVT) effect, is hampered by graft-versus-host disease (GVHD) and consequent treatment-related mortality. In this study, we demonstrated that ruxolitinib, a JAK1/JAK2 inhibitor, abrogates acute GVHD while sparing the GVT effect. This effect is associated with preserved alloreactivity *in vivo* and reduced T-cell infiltration of GVHD target organs. Ruxolitinib is approved by the FDA and The European Medicines Agency (EMEA) for the treatment of patients with myelofibrosis, and Janus-activated kinase (JAK) signaling and JAK2 inhibitors play an important role in myeloid and lymphoid malignancies. Thus, these data add to the body of evidence that JAK2 inhibition may represent a new and potentially clinically relevant approach to GVHD prevention. Furthermore, the antitumor effect of this compound may allow inhibiting GVHD while controlling tumor burden, which is an important step toward more effective treatment of patients with hematologic malignancies.

Another report suggested a role for JAK1/JAK2 modulation to reduce GVHD and improve survival in a mouse model of allogeneic transplant (19).

Given the importance of JAK signaling and its inhibitors in the contest of myeloid and lymphoid malignancies (12, 20, 21) and because JAK1/JAK2 inhibition might represent a more specific and narrow form of immune modulation relative to standard approaches of immune suppression, we reasoned that ruxolitinib may be a promising drug to be tested in order to preserve GVT and obtain an anti-GVHD effect with a potential fast track for translation into clinical trials. We tested our hypothesis in a mouse model of acute GVHD comprising inoculation of two different tumor cell lines.

## Materials and Methods

### Animals

Female C57BL/6 (B6, H-2K$^b$) and BALB/c (H-2K$^d$) mice were obtained from Charles River Laboratories. Mice were maintained in a specific pathogen-free facility, and treated according to an animal protocol that was approved from CESA (Comitato Etico per la Sperimentazione Animale) of the University of Milan (Milan, Italy) and from the Ethical Committee (study number: INT_21/09) of the Fondazione IRCCS Istituto Nazionale dei Tumori (Milan, Italy).

### Cell preparations

B6 bone marrow and spleen cells were purified by magnetic bead-negative depletion in an autoMACS Pro Separator (Miltenyi Biotec) to obtain a purity of 95% to 98%. In detail, donor bone marrow was T cell depleted (TCD) by Miltenyi CD90 [Thy1.2] microbeads, and splenic donor T cells were purified with Miltenyi CD45R [B220] microbeads. Lymphoma A20 cell line was kindly provided from Dr M.P. Colombo's laboratory (Molecular Immunology Unit at the Fondazione IRCCS Istituto Nazionale dei Tumori, Milan, Italy) >6 months after being purchased from a cell bank. Myeloid leukemia RMB-1 cell line was purchased from DMSZ and was confirmed as murine with isoelectric focusing (IEF) of aspartate aminotransferase (AST), lactate dehydrogenase (LDH), malic dehydrogenase (MDH), nucleoside phosphorylase (NP). No authentication was done in our laboratory. Both A20 and RMB-1 cell lines are of H2K$^d$-positive phenotype. Tumor cells were cultured in complete medium (CM) consisting of RPMI-1640 (Lonza), 10% FCS (Sigma), and Pen–Strep 100 U/mL (Sigma). Tumor-cell lines were cocultured with/without ruxolitinib at the concentration of 10 μmol/L for 24 hours; cell viability was checked by flow cytometry analysis with PI and Annexin V (Miltenyi Biotec).

### Bone marrow transplantation and tumor cell inoculation

Recipient BALB/c mice were lethally irradiated (950 Gy total dose by two separate doses 3 hours apart) and reconstituted by intravenous (i.v.) injection of TCD B6 bone marrow cells ($10 \times 10^6$ cells) alone or with the addition of purified B6 T cells ($2{,}5 \times 10^6$ cells). As per our animal protocol, any transplant recipient that was premorbid (defined by >30% loss in body weight or severe loss in activity) was euthanized. In our facility, this mouse model of GVHD resulted in limited lethality, with only a fraction of the mice dying at later time points (from days 30 to 60). A20 or RMB-1 cells were injected i.v. on day 0 of transplant at the dosage of $2 \times 10^6$ cells and $0.5 \times 10^6$ cells, respectively.

### Ruxolitinib treatment

Mice treated with ruxolitinib (INCB018424; Selleck Chemicals) received the pharmacologic inhibitor of the JAK1–JAK2 pathway twice-daily by oral gavage from the day of transplant to day 14 after bone marrow transplantation (BMT). Ruxolitininb was solubilized in DMSO and resuspended in water containing 0. 5% methylcellulose and 5% N,N-dimethylacetamide to a final volume of 200 μL, as previously described (22). Initial drug dosage, 90 mg/kg/d, was mutated from previous publication where it was used in a mouse model of myeloproliferative disease (22). Other dosages comprised 45 and 22.5 mg/kg/d, as described in the Results.

### Histology

For histopathologic grading of GVHD lesions, mice from each cohort were killed at day 14 post-BMT and skin, liver, small intestine, and large intestines were harvested. Tissues were fixed in 10% neutral buffered formalin and paraffin embedded. Tissue sections were routinely stained with hematoxylin and eosin (H&E) and evaluated in a blinded fashion under a light microscope. Skin, liver, small and large intestine were scored semiquantitatively, as previously described (Supplementary Fig. S1; ref. 23). Scores of the individual organs (range, 0–4) were then added to provide a total GVHD score for each mouse (range, 0–16).

### Immunohistochemistry

To establish the extent of T-cell and macrophage infiltration in GVHD target organs, formalin-fixed and paraffin-embedded sections from skin, liver, and ileum were immunostained with CD3-epsilon (M20; Santa Cruz Biotechnology) and IBA-1 (Wako)-specific antibodies, and five fields at ×400 were selected from within the major sites of inflammatory lesions. For each field, the number of CD3-epsilon$^+$ T cells and IBA-1$^+$ macrophages was counted using the ImageJ analysis program (http://rsb.info.nih.gov/ij/).

### Flow cytometry analysis

Spleen and bone marrow were harvested on day 14 post-BMT, and single-cell suspensions were labeled with anti-CD62L, -H-2K$^b$ (BioLegend), -CD3, -CD8, -CD4, and -CD44 (Miltenyi Biotec) conjugated with FITC, PE, VioBlue, PerCP, APC-Vio770, and PE-Vio770, respectively. For regulatory T cells (Treg) quantification, spleen cells were fixed and permeabilized with the Foxp3 staining buffer set (Miltenyi Biotec) and labeled with anti-H-2K$^b$, -CD25, -CD127 (BioLegend), -Foxp3, -CD3, -CD4 (Miltenyi Biotec) conjugated with FITC, PE, PeCy7, APC, VioBlue, and APC Vio770. A20 tumor cells were identified both in the spleen and bone marrow by FSC/SSC characteristics together with the following antibodies: anti-H-2K$^d$-FITC, B220-VioBlue, and CD3-APC (Miltenyi Biotec). RMB1 tumor cells were followed both in the spleen and bone marrow by labeling them with anti-H-2K$^d$-FITC (BioLegend), CD11b-Vio-Blue, Gr1-and PerCP Vio770 (Miltenyi Biotec). Six- to seven-color flow cytometry was performed on a MACSQuant Analyzer (Miltenyi Biotec) using MACSQuantify 2.4 software (Miltenyi Biotec).

For mixed lymphocyte reaction experiments, posttransplant splenic single cells were adjusted to $0.5 \times 10^6$ cells/mL and either not stimulated or stimulated with B6 DC, or BALB/c DCs generated by culturing marrow cells for 6 days in rmGM-CSF and rmIL4 (each at 1,000 IU/mL; PeproTech); bacterial lipopolysaccharide (LPS; 1 μg/mL; Sigma) was added to the final 24 hours of DC culture. Expanded DCs were washed and used at a spleen cell to DC ratio of 10:1. After 24 hours, cells were evaluated by intracellular flow cytometry for IFNγ secretion capacity by first permeabilization with the Inside Stain kit (Miltenyi Biotec) and subsequent labeling with anti-H-2K$^b$-FITC (BioLegend), CD4-VioBlue, CD8-PerCP, and IFNγ-PE (Miltenyi Biotec). Allospecific values were expressed in percentage of cells positive for IFNγ secretion and calculated after adjusting for values obtained after stimulation with syngeneic B6 DC.

For quantification of IL17 secretion capacity, single-cell suspension from spleens was activated with PMA (100 ng/mL; Sigma) and ionomycin (1 μg/mL; Sigma) for 3 hours and incubated with brefeldin (Sigma) for another 4 hours. Cells were permeabilized with the Inside Stain Kit (Miltenyi) and stained with anti-H-2K$^b$-FITC (BioLegend), CD4-VioBlue, CD8-PerCP, IL17 APC (Miltenyi Biotec).

For blood cell analysis, blood samples were collected by retro-orbital venipuncture on day +14 and +30 post-BMT and labeled with CD3 FITC, Gr-1 PerCP, Ter119 APC, and B220 VioBlue (Miltenyi Biotec).

### ELISA

On day 14 post-BMT, serum was collected from transplanted mice by retro-orbital bleeding. Cytokine production was evaluated using 2-site ELISAs (IL6 and IL12 quantikine ELISA kit purchased from R&D Systems).

### Statistical analysis

Survival analysis was performed according to the Kaplan–Meier method, and survival curves were compared using the log-rank testing. Flow and cytokine data were analyzed using the Student two-tailed $t$ tests. Values of $P < 0.05$ were considered statistically significant.

## Results

### Ruxolitinib abrogates acute GVHD *in vivo*

First, we evaluated whether ruxolitinib inhibited acute GVHD *in vivo* using a fully MHC-mismatched mouse model of BMT (23). We tested ruxolitinib at 90 mg/kg/d: data shown are from three independent experiments comprising 10 to 15 mice per cohort. All experimental cohorts had an initial weight loss due to radiation toxicity (Fig. 1A). Thereafter, mice receiving only TCD bone marrow (BM) cells ("BM only") had a full recovery of their weight, whereas mice in the GVHD group treated with vehicle only ("GVHD+Vehicle") had a slow and constant reduction of their weight up to −30% on day 48 post-BMT. Treatment with ruxolitinib for 14 days posttransplant (GVHD+ruxolitinib) was associated with an initial additional weight loss and a subsequent slow recovery of weight back to levels reached by the "BM only" cohort. Histologic analysis at day 14 post-BMT revealed reduced lesions of GVHD in all organs of ruxolitinib-treated mice (Fig. 1B), including skin ($P < 0.0001$), liver ($P = 0.001$), small ($P < 0.0001$) and large intestines ($P < 0.0001$; Fig. 1C). Unexpectedly, liver examination revealed moderate centrilobular hepatocellular hypertrophy (Fig. 1D), compatible with hepatic toxicity in ruxolitinib-treated animals. In conclusion, ruxolitinib is capable of preventing weight loss and end-organ pathologic changes associated with acute GVHD; however, ruxolitinib therapy caused potential adverse effects at the dose of 90 mg/kg/d, as revealed by hepatic toxicity and early weight loss.

### Ruxolitinib treatment has a dose-dependent effect on acute GVHD reduction

Next, we characterized whether reduction of ruxolitinib dosage may abrogate acute GVHD, while sparing mice from adverse drug effects. To test this hypothesis, recipients were treated orally with ruxolitinib at 90 mg/kg, 45 mg/kg, or 22.5 mg/kg per day, respectively: results were combined from at least three different experiments with 12 to 15 recipients per cohort (Fig. 2). Mice receiving ruxolitinib at 45 mg/kg/d had significant improvement of overall survival (OS) relative to GVHD controls ($P = 0.03$) and relative to ruxolitinib recipients at the 90 mg/kg/d dose ($P = 0.01$; Fig. 2A). Ruxolitinib at both the 90 and 45 mg/kg/d dosing yielded less weight loss relative to the GVHD cohort (Fig. 2B). The beneficial effect of ruxolitinib was partially lost when the drug was administered at the further reduced dose of 22.5 mg/kg/d, as documented by both survival curves and weight changes (Fig. 2A and B). Histologic analysis at day 14 post-BMT confirmed reduced lesions of GVHD in the examined organs of ruxolitinib-treated mice (Fig. 2C), with a dose-dependent effect of ruxolitinib on GVHD pathology score of skin, small and large intestines. Ruxolitinib delivered at 90 and 45 mg/kg daily doses was effective in this regard, whereas the 22.5 mg/kg dose was only nominally effective against histologically defined GVHD (Fig. 2D). Histologic evidence of GVHD in the liver was relatively refractory to ruxolitinib therapy, as there existed residual presence of portal inflammatory infiltrates still visible at the dose level of 90 mg/kg (Fig. 2C and D). Moreover, we detected a similar dose-dependent effect of ruxolitinib on proinflammatory cytokine production: relative to vehicle-treated mice, posttransplant IL6 levels were significantly reduced at all three ruxolitinib doses ($P < 0.05$); however, the most significant reductions occurred at the 90 and 45 mg/kg/d doses rather than the 22.5 mg/kg/d dose ($11.7 \pm 0.1$ vs.

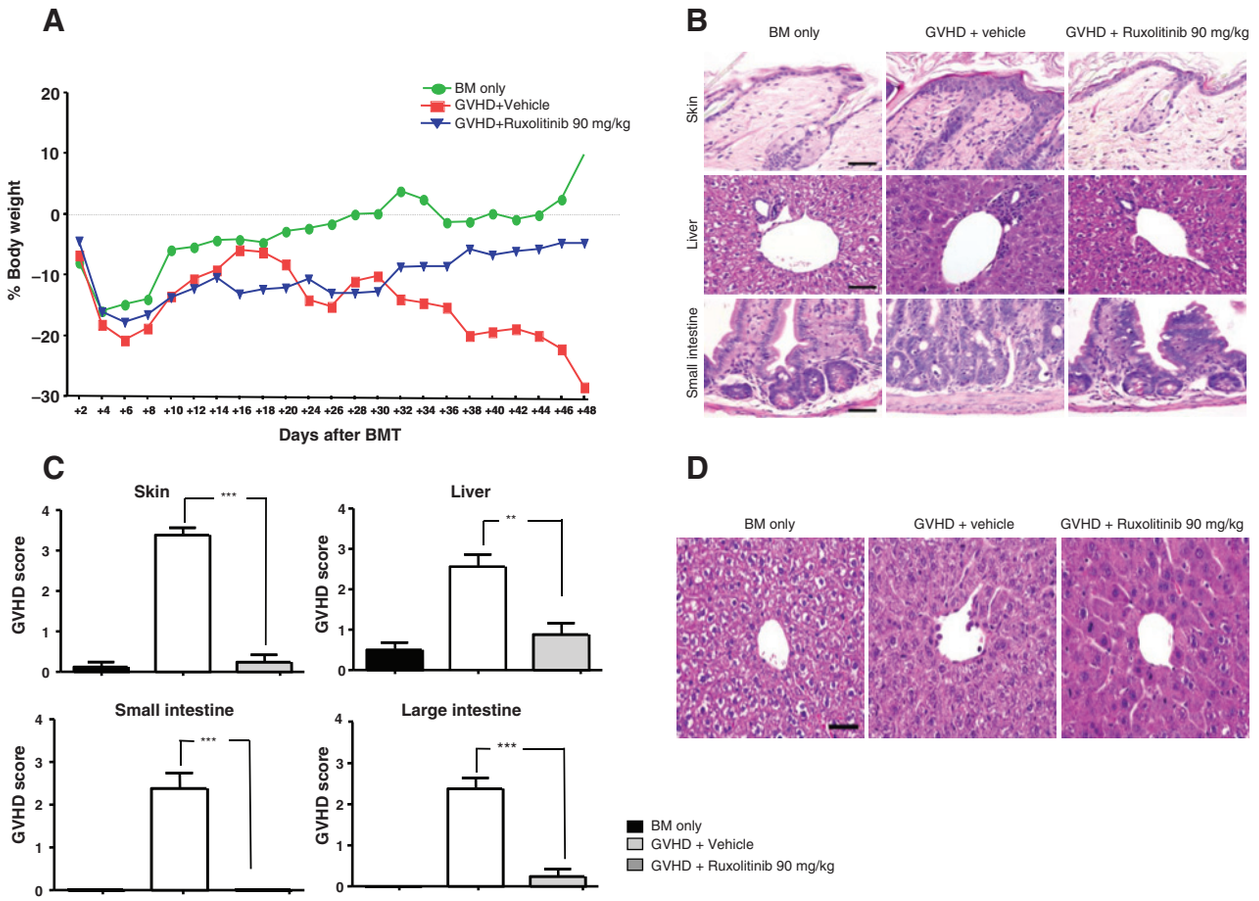


**Figure 1.**
Ruxolitinib abrogates acute GVHD after allogeneic BMT. BALB/c recipient mice were lethally irradiated (950 Gy) and transplanted with donor B6 cells consisting of $10 \times 10^6$ TCD-BM cells alone (BM only) or with $2.5 \times 10^6$ T cells (GVHD). From day 0 to day 14 post-BMT, mice were treated with vehicle only (GVHD+vehicle) or with ruxolitinib 90 mg/kg/d (GVHD+ruxolitinib 90 mg/kg) administered in two separate doses by oral gavage. A, recipient mice were monitored for weight change expressed as percentage of the pretransplant weight. Data were pooled from four independent experiments ($n = 10$–15 recipients per each cohort). B, recipient mice were sacrificed on day 14 post-BMT and liver, skin, small and large intestine were harvested to assess GVHD. Representative images of histologic sections of skin, liver, and small intestine are shown: H&E staining. C, for GVHD, each organ was scored on a scale of 0 to 4. Data were pooled from two independent experiments (at least $n = 6$ subjects for each cohort). D, representative images of histologic sections of liver, photographed at level of the centrilobular region. Centrilobular hepatocellular hypertrophy was evident in mice treated with ruxolitinib 90 mg/kg, suggestive of liver toxicity. Leucocyte adhesion to the endothelium of the centrilobular vein was present in GVHD + vehicle mice (middle), but absent in BM only (left), and GVHD + ruxolitinib 90 mg/kg (right) mice. *, $P < 0.05$; **, $P < 0.005$; ***, $P < 0.0001$.

15.9 ± 2.0 vs. 32.0 ± 1.0 pg/mL, $P < 0.05$). In summary, the best effect of ruxolitinib against GVHD was reached with 90 and 45 mg/kg/d, while a reduced benefit was observed at 22.5 mg/kg/d. Consistent with the existing literature (18, 22), we observed no significant effect of daily administration of ruxolitinib on post-BMT donor blood counts (Supplementary Fig. S2A–S2D). Indeed, relative to GVHD controls, treatment with ruxolitinib at 45 mg/kg/d was associated with improved myeloid and B-cell reconstitution on day 30 post-BMT. Of note, we found that, relative to the "BM only" cohort, ruxolitinib treatment was associated with similar myeloid and erythroid reconstitution, but reduced B-cell counts. C57BL/6 bone marrow cell engraftment was not delayed by ruxolitinib because the percentage of spleen $H2Kb^+$ cells was similar on day 14 between GVHD controls and mice treated with ruxolitinib at 90 or 45 mg/kg/d (92.2 ± 1.2 vs. 89.5 ± 1.7 vs. 95.1 ± 1.9, respectively; $P = 0.2$) and improved relative to the "BM only" cohort (72.6 ± 5.2, $P < 0.01$).

### During ruxolitinib treatment the GVT effect is maintained

We next evaluated whether ruxolitinib could abrogate acute GVHD without affecting the GVT effect. To test the hypothesis, in two separate experiments, we inoculated mice with A20 murine B-cell lymphoma cell line and analyzed the effect of ruxolitinib at the dose of 45 mg/kg. As expected, recipients of A20 and TCD-BM (BM only+A20) began to die of tumor starting from day 10 posttransplant. In marked contrast, all mice receiving allogeneic T cells treated with vehicle (GVHD+A20+vehicle) or with ruxolitinib (GVHD+ A20+ruxolitinib, 45 mg/kg dose) were alive on day 48 post-BMT ($P = 0.04$ and $P = 0.01$, respectively; Fig. 3A).

Because the antitumor effect may be related to a direct effect of the drug, we checked spleen and bone marrow for infiltration by A20 lymphoma cells in recipients of T cell-replete or TCD transplants that were further treated with posttransplant ruxolitinib. Percentages of A20 tumor cells infiltrating the spleen or bone marrow of recipients were similar in mice receiving TCD-BM

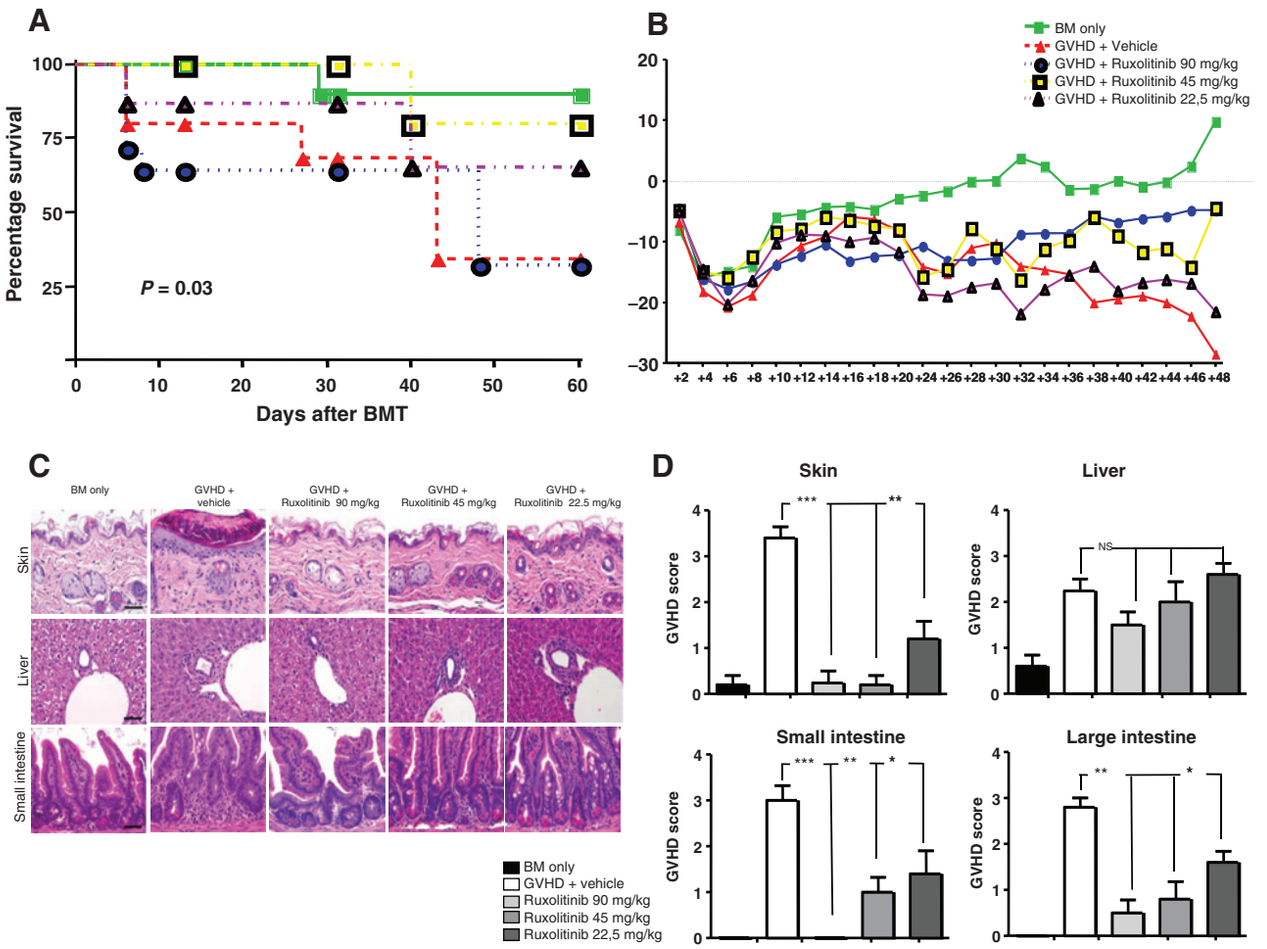


**Figure 2.**
Ruxolitinib effect on acute GVHD is dose-dependent. Lethally irradiated (950 Gy) BALB/c mice were transplanted with $10 \times 10^6$ B6 TCD-BM cells alone (BM only) or with $2.5 \times 10^6$ T cells and treated with vehicle (GVHD+vehicle) or ruxolitinib administered at 90 mg/kg/d (GVHD+ruxolitinib 90 mg/kg), 45 mg/kg/d (GVHD+ruxolitinib 45 mg/kg) or 22.5 mg/kg/d (GVHD+ruxolitinib 22.5 mg/kg), from day 0 to day 14 post-BMT. Data were pooled at least three independent experiments results are shown as mean ± SEM ($n$ = 12–15 per cohort). A, the Kaplan–Meier survival curve is shown. B, percentage weight change was expressed as percentage of the pretransplant weight. C, recipient mice were sacrificed on day 14 post-BMT and liver, skin, small and large intestine were harvested to assess GVHD. Representative images of histologic sections of skin, liver, and small intestine are shown: H&E staining. D, for GVHD each organ was scored on a scale of 0 to 4. Data were pooled from two independent experiments (at least $n = 5$ subjects for each cohort). *, $P < 0.05$; **, $P < 0.005$; ***, $P < 0.0001$.

alone (BM only+A20+vehicle) or with the addition of ruxolitinib (BM only+A20+ruxolitinib; Fig. 3B, left, and 3C). In marked contrast, recipients of allogeneic T cells with vehicle (GVHD+A20+vehicle) had a dramatic reduction of A20 lymphoma cells; this effect was fully preserved in mice treated with ruxolitinib (GVHD+A20+ruxolitinib; Fig. 3B, right and 3C; $P = 0.001$). These findings were further corroborated by *in vitro* experiments that evaluated cultured A20 tumor cells with or without ruxolitinib; no direct effect of the drug was observed on tumor cell-viability (data not shown). In a separate experiment, we tested whether the GVT effect was maintained against a different tumor cell line, the murine acute leukemia RMB-1. We observed that the percentages of spleen and bone marrow infiltration by RMB-1 cells were similar in the GVHD+vehicle and GVHD+ruxolitinib ($P = 0.1$ and $P = 0.2$, respectively) cohorts and significantly reduced compared with mice receiving RMB-1 cells with vehicle only ($P < 0.05$; Supplementary Fig. S3). As such, ruxolitinib therapy allowed for a GVT effect against both the A20 and RMB-1 cell lines.

### Ruxolitinib treatment was not associated with reduced alloreactivity

Given the preserved GVT effect, we wanted to analyze the effect of ruxolitinib on donor T-cell function. Previously, JAK-2 inhibition *in vitro* yielded significant reduction of T cell alloreactivity (18); however, the *in vivo* effect of JAK-2 inhibition has only partially been investigated (24). Data shown are combined from four different experiments with at least 15 to 20 mice per cohort. First, we found that administration of ruxolitinib at 45 mg/kg/d was not associated with a significant reduction of total spleen cells, including a full preservation of donor T cells ($P = 0.8$; Fig. 4A). Of note, the higher dose of ruxolitinib (90 mg/kg/d) yielded a significant reduction of spleen size and total cell number (Supplementary Fig. S4A); this result was consistent with

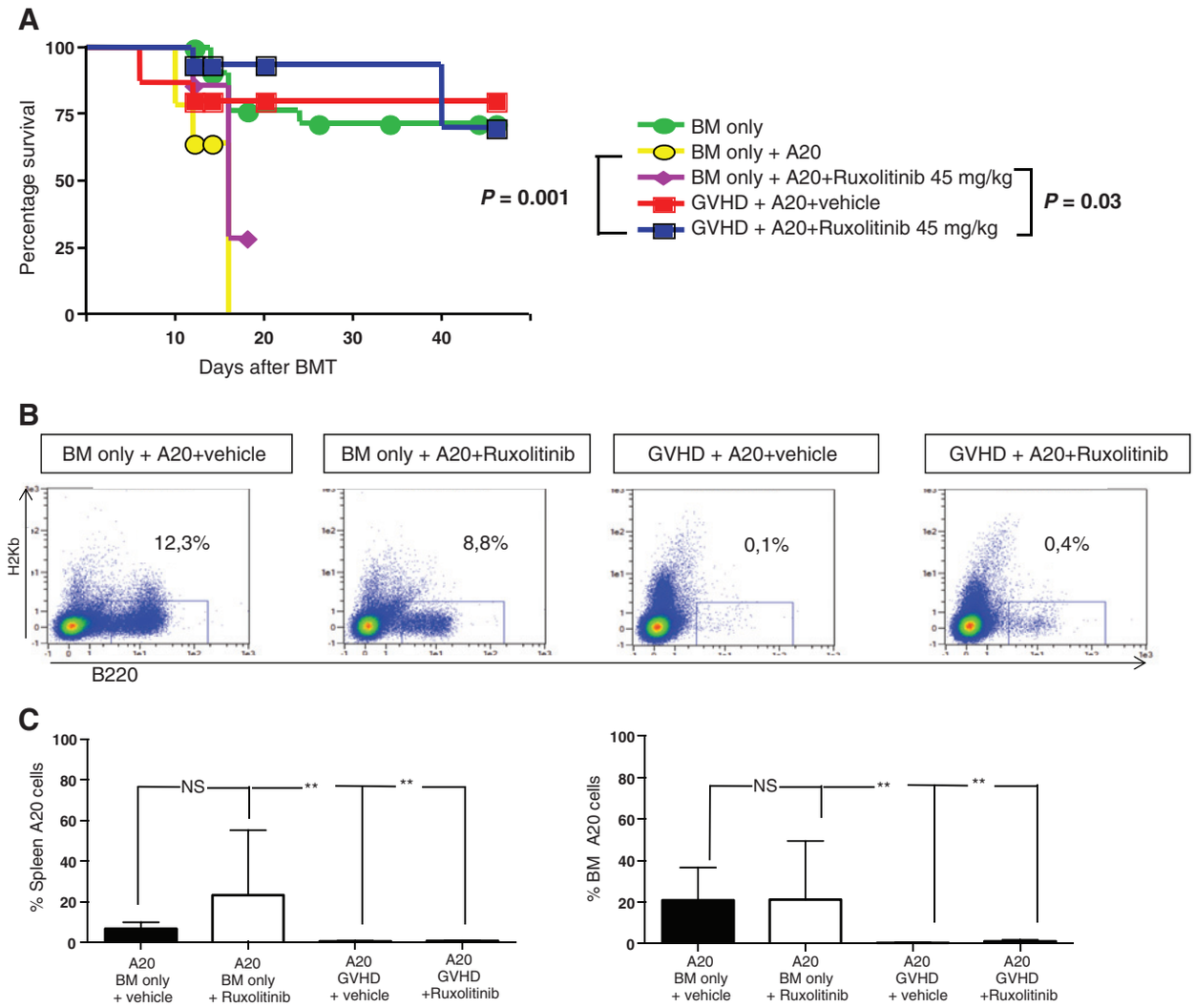


**Figure 3.**
Ruxolitinib prevents GVHD while maintaining a GVT effect. Lethally irradiated (950 Gy) BALB/c mice were transplanted with donor B6 cells consisting of $10 \times 10^6$ TCD-BM cells alone (BM only) or with $2.5 \times 10^6$ T cells with vehicle or with ruxolitinib at 45 mg/kg/d (GVHD+ruxolitinib 45 mg/kg) administered from day 0 to day 14 post-BMT. Additional mice were intravenously injected on the day of transplant with $2 \times 10^6$ A20 lymphoma tumor cells. Data were pooled from two separate experiments and results are shown as mean ± SEM (at least $n = 10$ per cohort). A, the Kaplan–Meier survival curve is shown. B, on day 14 post-BMT, spleen were isolated and analyzed by flow cytometry for A20 infiltration. Representative flow data are shown. C, data from two separate experiments were pooled to evaluate the effect of ruxolitinib alone or in the GVHD cohort on spleen and bone marrow infiltration by A20 lymphoma cells. Results are shown as mean ± SEM ($n = 10$ per cohort). *, $P < 0.05$; **, $P < 0.005$.

previous observations (22). Relative to T-cell differentiation, posttransplant ruxolitinib therapy yielded an increase of $CD62L^+CD44^+$ central memory (CM) T cells (10.8% ± 2.1% vs. 2.3% ± 0.3%; $P < 0.0001$) and reduction of $CD62L^-CD44^+$ effector memory (EF) T cells (87.2% ± 2.5% vs. 97.5% ± 0.3%; $P < 0.0001$; Fig. 4B). Similar results were obtained with ruxolitinib at 90 mg/kg/d ($P < 0.0001$; Supplementary Fig. S4B). Ruxolitinib did not induce a significant reduction of alloreactive T cells in terms of percentages of $CD4^+IFN\gamma^+$ (7.2% ± 0.8% vs. 5.6% ± 1.1%; $P = 0.2$) and $CD8^+IFN\gamma^+$ (7.1% ± 0.8% vs. 5.6% ± 0.6%; $P = 0.2$) cells (Fig. 4C) and in terms of absolute numbers of splenic $CD4^+IFN\gamma^+$ ($1.9 \pm 0.5 \times 10^5$ vs. $1.8 \pm 0.4 \times 10^5$; $P = 0.8$) and $CD8^+IFN\gamma^+$ cells ($3.3 \pm 0.7 \times 10^5$ vs. $2.6 \pm 0.6 \times 10^5$; $P = 0.4$; Supplementary Fig. S5A). Similar results were achieved when ruxolitinib was delivered at the highest dosage (Supplementary Fig. S4C). Of note, mice treated with ruxolitinib at 45 mg/kg had much higher percentages of alloreactive $CD4^+IFN\gamma^{++}$ and $CD8^+$ $IFN\gamma^+$ cells compared with control mice receiving only TCD-BM ($P = 0.0007$ and $P = 0.0002$, respectively; Fig. 4C). Given the role of IL6 for Th17 polarization, we analyzed whether ruxolitinib affected Th17 differentiation *in vivo*; we found no significant changes relative to vehicle-treated mice both in terms of percentage (0.7% ± 0.2% vs. 0.8% ± 0.2%; $P = 0.8$; Fig. 4D) and absolute numbers ($2.5 \pm 0.8 \times 10^5$ vs. $3.7 \pm 1.1 \times 10^5$; $P = 0.4$; Supplementary Fig. S5B) of $Th17^+$ cells. Because it was recently shown that ruxolitinib is associated with preserved Treg differentiation (24), we analyzed the effect of the drug *in vivo* on $CD4^+$ $CD25^+CD127^{dim}Foxp3^+$ cells. In our model, we did not observe a

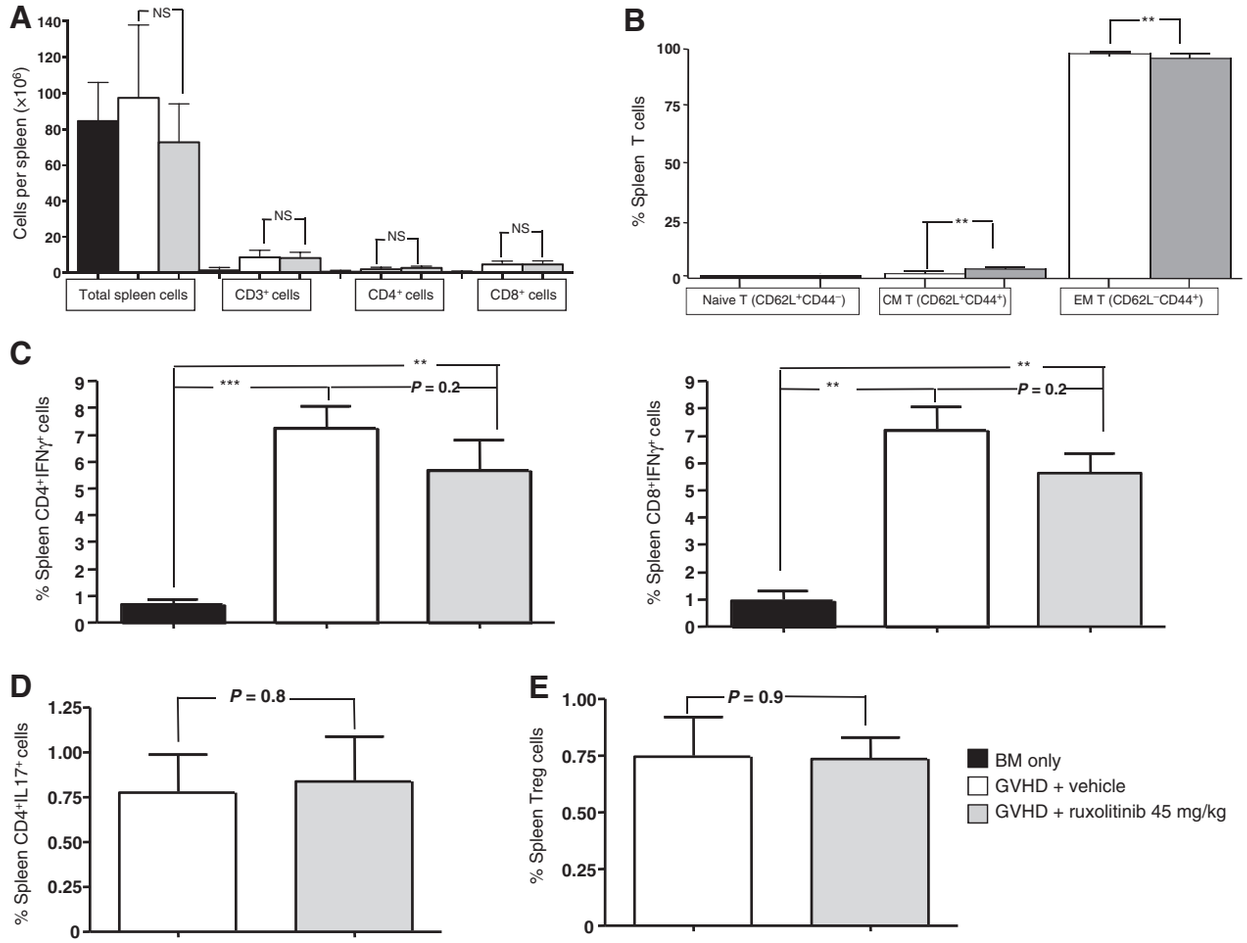


**Figure 4.**

Ruxolitinib prevents acute GVHD without abrogating T-cell alloreactivity. Lethally irradiated (950 Gy) BALB/c mice were transplanted with donor B6 cells consisting of $10 \times 10^6$ TCD-BM cells alone (BM only) or with $2.5 \times 10^6$ T cells plus vehicle (GVHD+vehicle) or ruxolitinib 45 mg/kg/d (GVHD+ruxolitinib 45 mg/kg) administered in two separate doses by oral gavage. Results were pooled from four different experiments and shown as mean ± SEM ($n = 10$–20 mice per cohort). On day 14 post-BMT, spleens were harvested and analyzed by flow cytometry for T-cell composition (A) and T-cell subsets to enumerate central memory (CM), effector memory (EF), and naïve T cells (B). Single-cell suspensions were: (C) stimulated with syngeneic or allogeneic DC and analyzed by intracellular flow cytometry to obtain percentages of host $CD4^+$ and $CD8^+$ cells producing allospecific IFNγ; (D) stimulated with PMA/ionomycin to evaluate percentages of $CD4^+$ cells capable of secreting IL17 by intracellular flow cytometry. E, spleen cells were also analyzed to detect percentage of $CD4^+CD25^+CD127^{dim}Foxp3^+$+Tregs out of the total $CD4^+$ cells. *, $P < 0.05$; **, $P < 0.005$; ***, $P < 0.0001$.

reduction of Tregs in ruxolitinib-treated mice in terms of percentages (0.7% ± 0.1% vs. 0.7% ± 0.09%; $P = 0.3$; Fig. 4E) and absolute numbers ($0.4 \pm 0.1 \times 10^5$ vs. $0.9 \pm 0.4 \times 10^5$; $P = 0.2$; Supplementary Fig. S5C) of $CD4^+CD25^+CD127^{dim}Foxp3$ T cells. Of note, we obtained similar results with the drug delivered at 22.5 mg/kg (data not shown) and 90 mg/kg (Supplementary Fig. S4C and S4D). In conclusion, suppression of acute GVHD by ruxolitinib at the dose of 45 mg/kg/d was not associated with a reduction in alloreactivity or modulation of the balance of Th17 and Tregs.

### Ruxolitinib treatment reduced overall T-cell infiltrates in GVHD organ sites

Because GVHD prevention can be achieved by modulation of T-cell migration to organ sites (25–27), we speculated that ruxolitinib may induce a reduced T-cell recruitment to GVHD targets. Indeed, the immunohistochemical quantification of T-cell (CD3 epsilon$^+$) infiltration into GVHD target organs at day 14 post-BMT revealed that treatment with ruxolitinib reduced T-cell numbers in the skin [number of intraepithelial (IEL) cells/skin length: 47 ± 5 vs. 2.5 ± 0.7; $P < 0.0001$; Fig. 5A], in the small intestine (number of $CD3^+$ cells/mucosa area: 882 ± 90 vs. 167 ± 112; $P < 0.0001$; Fig. 5B), and in the liver (IEL/bile duct area: 1,856 ± 27 vs. 674 ± 99; $P < 0.0001$; Fig. 5C). Moreover, given the importance of monocytes/macrophages activation for GVHD process (28), we analyzed macrophage (Iba-$1^+$) infiltration at GVHD sites and observed a similar reduction induced by ruxolitinib (Fig. 5A–C and Supplementary Fig. S6).

Because CXCR3 expression is known to support T-cell migration to the skin, gut, and liver in murine models of GVHD (29–31), we analyzed the effect of ruxolitinib on CXCR3 *in vivo*. Ruxolitinb prophylaxis significantly reduced the expression of CXCR3 both on splenic $CD4^+$ (88% ± 1% vs. 82% ± 1%; $P = 0.01$) and $CD8^+$ cells T cells (81% ± 1% vs. 64% ± 4%; $P =$

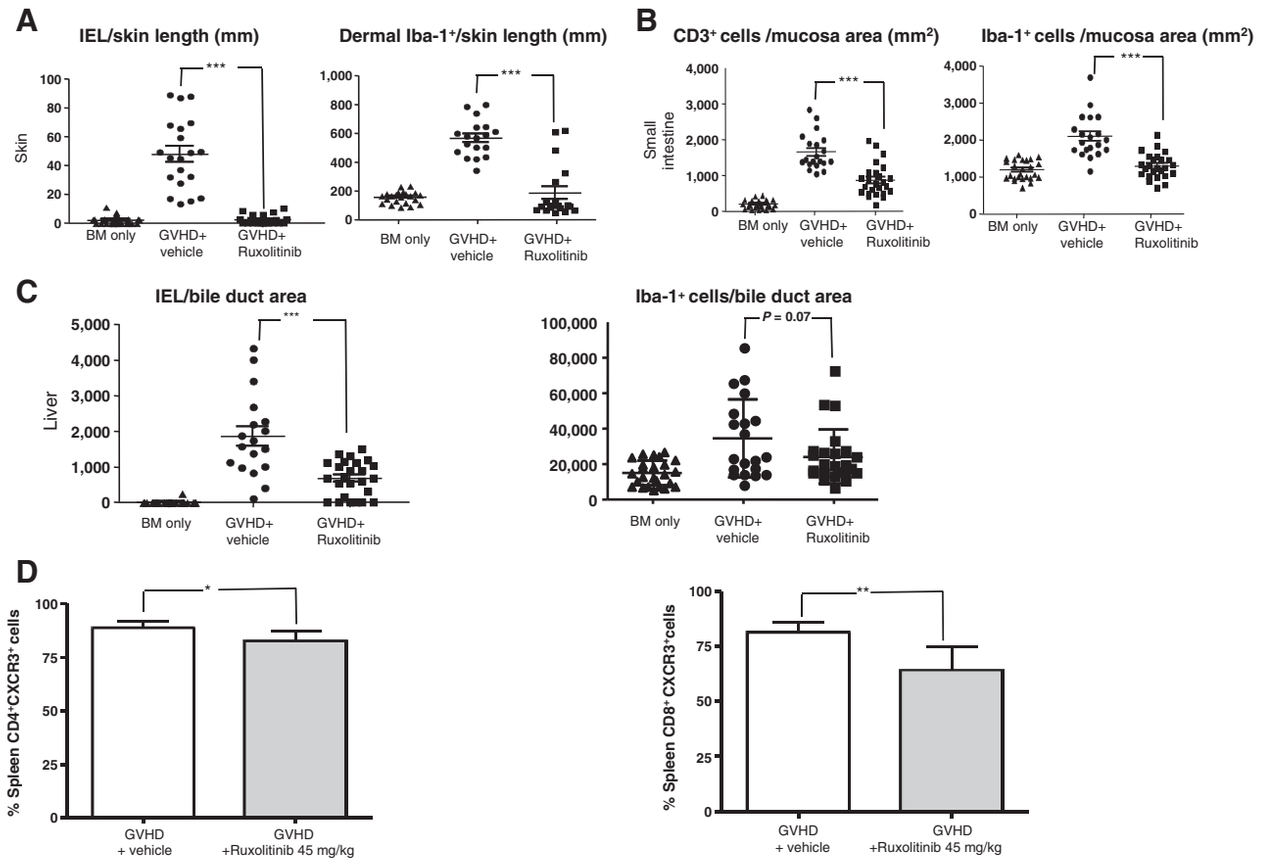


**Figure 5.**

Ruxolitinib reduces T-cell and macrophages migration to GVHD target organs. Lethally irradiated (950 Gy) BALB/c mice were transplanted with $10 \times 10^6$ B6 TCD-BM cells alone (BM only) or plus $2.5 \times 10^6$ T cells and treated with vehicle (GVHD+vehicle) or ruxolitinib at 45 mg/kg/d (GVHD+ruxolitinib 45 mg/kg) administered from day 0 to day 14 post-BMT. Data were pooled from three separate experiments and results are shown as mean ± SD ($n = 20$–25 per cohort). A–C, quantification of T cells and macrophages infiltrating the examined organs. Recipient mice were sacrificed on day 14 post-BMT and liver, skin, and small intestines were harvested. T cells and macrophages infiltrates were identified by CD3-epsilon and Iba-1 immunostaining of formalin-fixed and paraffin-embedded sections. For each sample, the number of CD3-epsilon$^+$ and Iba-1$^+$ cells was evaluated in five fields photographed at ×400 magnification. Results are presented as the ratio between the cell count and skin length (mm), bile duct area (mm$^2$), sublobular/centrilobular vein perimeter (mm), and intestinal mucosa area (mm$^2$), respectively. Bars show the mean ± SD. D, spleen cells were isolated on day 14 post-BMT and analyzed by flow cytometry for CXCR3 expression on CD4$^+$ and CD8$^+$ cells. *, $P < 0.05$; **, $P < 0.005$; ***, $P < 0.0001$.

0.004; Fig. 5D). Interestingly and in agreement with a supposed effect of the drug on T-cell migration to target sites, we have also found that discontinuation of ruxolitinib treatment on day 14 lead to an initial recurrence of GVHD on day 30 posttransplant (data not shown).

## Discussion

The ideal scenario of allogeneic-HSCT in patients with hematologic malignancies is to promote an immune-mediated GVT effect while preventing the occurrence of GVHD. Acute and chronic GVHD still represent an important complication and the main causes of nonrelapse mortality after transplant (3, 32). In this report, we showed in a mouse model of fully MHC-mismatched BMT that pharmacologic modulation of the JAK1–JAK2 pathway by ruxolitinib is capable of maintaining the GVT activity while reducing GVHD. Although the precise mechanism of this separation of GVHD from GVT effects will require further investigation, our results indicate that ruxolitinib may operate by preserving alloreactivity (thus allowing a GVT effect) while simultaneously modulating T-cell homing (thus allowing a modulation of GVHD).

Our findings may have important implications for clinical application of ruxolitinib in the contest of allogeneic HSCT. First, ruxolitinib is now available in clinic and is currently used for patients with myelofibrosis (9); this contest may facilitate a fast track for clinical trials evaluating ruxolitinib in the transplant setting. Of note, in our preclinical model, ruxolitinib was safe and not associated with hematologic toxicity. Second, JAK–STAT signaling was recently shown to have a strong relevance not only for the pathogenesis of myeloproliferative diseases, but also for the outcome of patients with diffuse-large B-cell lymphomas where pSTAT3 expression was associated with a poor outcome (33). Moreover, a new JAK2/FLT3 inhibitor, pacritinib, has recently shown promising results both in xenograft mouse models of JAK2$^{V617F}$-driven diseases (20) and in patients with relapsed lymphoma (21). These recent acquisitions suggest a potential intriguing

applicability of posttransplant pharmacologic modulation of JAKs in order to both inhibit GVHD and control tumor burden by a drug-mediated effect or by making myeloid and lymphoid diseases more susceptible to allo-responses. Importantly, we found that ruxolitinib not only yields significant anti-GVHD activity, but also preserves the GVT effect against two different tumor cell lines and that this was not due to a direct antitumor effect but rather was likely the result of a sustained posttransplant T-cell alloreactivity. This is consistent with the fact that A20-mediated malignancy is driven by NF-κB activation rather than JAK–STAT signaling (34); consistent with this biology, we observed initial recurrence of GVHD at target sites on day +30 post-BMT after suspending ruxolitinib. Therefore, our results suggest that patients with a broad spectrum of hematologic malignancies may benefit from treatment with ruxolitinib after transplant.

In this study, we provide further strength to the recent findings by Choi and colleagues (35): that is, pharmacologic inhibition of the JAK1–JAK2 pathway by ruxolitinib was associated with a preserved GVT effect. Building upon this prior study, we now show that the preserved GVT activity by ruxolitinib is associated with maintained *in vivo* polarization of donor T cells toward the Th1 and Th17 phenotypes that are generally recognized as efficient mediators of antitumor effects (36, 37). Moreover, our observations are in agreement with a previous report from Choi and colleagues (19) that described JAK1/JAK2 inhibition by ruxolitinib as an approach to block the IFNγR–CXCR3 axis and prevent T-cell migration into GVHD organs. Indeed, we also found a reduction of CXCR3 expression, but this effect was more evident on $CD8^+$ cells, and limited on $CD4^+$ subsets. This modest effect of ruxolitinib on chemokine expression in our model suggests that other factors may have contributed to the reduced overall infiltration of donor T cells in the GVHD target tissues. Given the pathophysiologic three-step model of acute GVHD (38), reduced tissue infiltration may also have been a result of reduced alloreactivity and T-cell proliferation. For instance, Betts and colleagues (18) showed that JAK2 inhibition reduced DC-mediated T-cell activation, thereby impairing the activation of central and effector memory T cells as well as the expansion of responder Th1 and Th17 cells. We did not investigate DC activation in this study, but the fact that spleen T-cell infiltration, circulating T-cell numbers, Th1 and Th17 polarization were unchanged in mice receiving ruxolitinib suggests that this might not be the most relevant mechanism in our mouse model.

Of note, prevention of acute GVHD in our experiments was more pronounced in the skin and the intestine. Whether this effect was due to a different modulation of chemokines involved in liver GVHD, such as CXCR6 (39) and CCR5 (40), would be the object of further investigations. Interestingly, our findings partially confirm and also extend a recent study by Spoerl and colleagues (24) who reported a similar anti-GVHD effect of ruxolitinib in a mouse model of transplant. In fact, we demonstrated that ruxolitinib could preserve an immunologic GVT effect, but, differently from the earlier report, we could not identify increased Treg differentiation *in vivo*. It is possible that methodologic differences between the two experimental models may explain the fact that potential mechanisms of ruxolitinib mechanism of action against GVHD were identified.

In conclusion, our work provides further rationale for evaluating the effect of ruxolitinib on GVHD and GVT effects in clinic trials for patients with hematologic malignancies undergoing allogeneic HSCT. Although our findings point to chemokine modulation as a potential mechanism of action, further mechanistic studies will be required to better understand the precise mechanism of action of ruxolitinib for GVHD prevention. Our results open the way to test the potential application of new JAK inhibitors, such as pacritinib, both for regulating GVHD and directly inhibiting lymphoma cell proliferation after HSCT.

## Disclosure of Potential Conflicts of Interest

No potential conflicts of interest were disclosed.

## Authors' Contributions

**Conception and design:** C. Carniti, P. Corradini, J. Mariotti
**Development of methodology:** C. Carniti, P. Corradini, J. Mariotti
**Acquisition of data (provided animals, acquired and managed patients, provided facilities, etc.):** C. Carniti, S. Gimondi, A. Vendramin, D. Confalonieri, P. Corradini, J. Mariotti
**Analysis and interpretation of data (e.g., statistical analysis, biostatistics, computational analysis):** C. Carniti, S. Gimondi, A. Vendramin, C. Recordati, P. Corradini, J. Mariotti, D. Confalonieri
**Writing, review, and/or revision of the manuscript:** C. Carniti, C. Recordati, P. Corradini, J. Mariotti
**Administrative, technical, or material support (i.e., reporting or organizing data, constructing databases):** A. Bermema
**Study supervision:** C. Carniti, P. Corradini, J. Mariotti

## Acknowledgments

The authors thank Dr. Daniel Fowler of the Experimental Transplantation and Immunology Branch, NCI, for critical revision of the article and valuable comments.

## Grant Support

This study was supported by the Italian Association for Cancer Research (AIRC) with My First AIRC grant number 11936 and the European Union for Marie Curie reintegration grant number 268113.

The costs of publication of this article were defrayed in part by the payment of page charges. This article must therefore be hereby marked *advertisement* in accordance with 18 U.S.C. Section 1734 solely to indicate this fact.

Received October 28, 2014; revised January 29, 2015; accepted May 1, 2015; published OnlineFirst May 14, 2015.

## References

1. Appelbaum FR, Forman SJ, Negrin RS, Blume KG. Thomas' Hematopoietic Cell Transplantation: Stem Cell Transplantation. 4th ed. Wiley-Blackwell, Oxford, UK, 2011.
2. Baron F, Storb R. Allogeneic hematopoietic cell transplantation following nonmyeloablative conditioning as treatment for hematologic malignancies and inherited blood disorders. Mol Ther 2006;13:26–41
3. Pavletic SZ, Fowler DH. Are we making progress in GVHD prophylaxis and treatment? Hematology Am Soc Hematol Educ Program 2012;2012:251–64.
4. Fowler DH. Shared biology of GVHD and GVT effects: potential methods of separation. Crit Rev Oncol Hematol 2006;57:225–44.
5. Blazar BR, Murphy WJ, Abedi M. Advances in graft-versus-host disease biology and therapy. Nat Rev Immunol 2012;12:443–58.
6. Reshef R, Luger SM, Hexner EO, Loren AW, Frey NV, Nasta SD, et al. Blockade of lymphocyte chemotaxis in visceral graft-versus-host disease. N Engl J Med 2012;367:135–45.
7. Baxter EJ, Scott LM, Campbell PJ, East C, Fourouclas N, Swanton S, et al. Acquired mutation of the tyrosine kinase JAK2 in human myeloproliferative disorders. Lancet 2005;365:1054–61
8. Savage KJ, Monti S, Kutok JL, Cattoretti G, Neuberg D, De Leval L, et al. The molecular signature of mediastinal large B-cell lymphoma differs from that

of other diffuse large B-cell lymphomas and shares features with classical Hodgkin lymphoma. Blood 2003;102:3871–9.
9. Ding BB, Yu JJ, Yu RY, Mendez LM, Mendez LM, Shaknovich R, et al. Constitutively activated STAT3 promotes cell proliferation and survival in the activated B-cell subtype of diffuse large B-cell lymphomas. Blood 2008;111:1515–23.
10. Holtick U, Vockerodt M, Pinkert D, Schoof N, Stürzenhofecker B, Kussebi N, et al. STAT3 is essential for Hodgkin lymphoma cell proliferation and is a target of tyrphostin AG17 which confers sensitization for apoptosis. Leukemia 2005;19:936–44.
11. Huang X, Meng B, Iqbal J, Ding BB, Perry AM, Cao W, et al. Activation of the STAT3 signaling pathway is associated with poor survival in diffuse large B-cell lymphoma treated with R-CHOP. J Clin Oncol 2013;31:4520–8.
12. Verstovsek S, Kantarjian H, Mesa R, Pardanani AD, Cortes-Franco J, Thomas DA, et al. Safety and efficacy of a JAK1 and JAK2 inhibitor, INCB018424, in myelofibrosis. N Engl J Med 2010;363:1117–27.
13. Ghoreschi K, Laurence A, O'Shea JJ. Janus kinases in immune cell signaling. Immunol Rev 2009;228:273–87.
14. Mariotti J, Foley J, Ryan K, Buxhoeveden N, Kapoor V, Amarnath S, et al. Graft rejection as a Th1-type process amenable to regulation by donor Th2-type cells through an interleukin-4/STAT6 pathway. Blood 2008;112: 4765–75.
15. Laurence A, Amarnath S, Mariotti J, Kim YC, Foley J, Eckhaus M, et al. STAT3 transcription factor promotes instability of nTreg cells and limits generation of iTreg cells during acute murine graft-versus-host disease. Immunity 2012;37:209–22
16. Ma H, Lu C, Ziegler J, Liu A, Sepulveda A, Okada H, et al. Absence of Stat1 in donor $CD4^+$ T cells promotes the expansion of Tregs and reduces graft-versus-host disease in mice. J Clin Invest 2011;121:2554–69
17. Nikolic B, Lee S, Bronson RT, Grusby MJ, Sykes M. Th1 and Th2 mediate acute graft-versus-host disease, each with distinct end-organ targets. J Clin Invest 2000;105:1289–98.
18. Betts BC, Abdel-Wahab O, Curran SA, St Angelo ET, Koppikar P, Heller G, et al. Janus kinase-2 inhibition induces durable tolerance to alloantigen by human dendritic cell-stimulated T cells yet preserves immunity to recall antigen. Blood 2011;118:5330–9.
19. Choi J, Ziga ED, Ritchey J, Collins L, Prior JL, Cooper ML, et al. IFN$\gamma$R signaling mediates alloreactive T-cell trafficking and GVHD. Blood 2012; 120:4093–103.
20. Hart S, Goh KC, Novotny-Diermayr V, Hu CY, Hentze H, Tan YC, et al. SB1518, a novel macrocyclic pyrimidine-based JAK2 inhibitor for the treatment of myeloid and lymphoid malignancies. Leukemia 2011;25: 1751–9.
21. Younes A, Romaguera J, Fanale M, McLaughlin P, Hagemeister F, Copeland A, et al. Phase I study of a novel oral Janus kinase 2 inhibitor, SB1518, in patients with relapsed lymphoma: evidence of clinical and biologic activity in multiple lymphoma subtypes. J Clin Oncol 2012;30:4161–7.
22. Quintás-Cardama A, Vaddi K, Liu P, Manshouri T, Li J, Scherle PA, et al. Preclinical characterization of the selective JAK1/2 inhibitor INCB018424: therapeutic implications for the treatment of myeloproliferative neoplasms. Blood 2010;115:3109–17.
23. Fowler DH, Kurasawa K, Smith R, Eckhaus MA, Gress RE. Donor CD4-enriched cells of Th2 cytokine phenotype regulate graft-versus-host disease without impairing allogeneic engraftment in sublethally irradiated mice. Blood 1994;84:3540–9.
24. Spoerl S, Mathew NR, Bscheider M, Schmitt-Graeff A, Chen S, Mueller T, et al. Activity of therapeutic JAK 1/2 blockade in graft-versus-host disease. Blood 2014;123:3832–42.
25. Serody JS, Burkett SE, Panoskaltsis-Mortari A, Ng-Cashin J, McMahon E, Matsushima GK, et al. T-lymphocyte production of macrophage inflammatory protein-1alpha is critical to the recruitment of CD8(+) T cells to the liver, lung, and spleen during graft-versus-host disease. Blood 2000;96: 2973–80.
26. Terwey TH, Kim TD, Kochman AA, Hubbard VM, Lu S, Zakrzewski JL, et al. CCR2 is required for CD8-induced graft-versus-host disease. Blood 2005; 106:3322–30.
27. Haarberg KM, Li j, Heinrichs J, Wang D, Liu C, Bronk CC, et al. Pharmacologic inhibition of PKC$\alpha$ and PKC$\theta$ prevents GVHD while preserving GVL activity in mice. Blood 2013;122:2500–11.
28. Teshima T, Ferrara JL. Understanding the alloresponse: new approaches to graft-versus-host disease prevention. Semin Hematol 2002;39:15–22.
29. Duffner U, Lu B, Hildebrandt GC, Teshima T, Williams DL, Reddy P, et al. Role of CXCR3-induced donor T-cell migration in acute GVHD. Exp Hematol 2003;31:897–902.
30. Villarroel VA, Okiyama N, Tsuji G, Linton JT, Katz SI. CXCR3-mediated skin homing of autoreactive CD8 T cells is a key determinant in murine graft-versus-host disease. J Invest Dermatol 2014;134:1552–60.
31. Wysocki CA, Panoskaltsis-Mortari A, Blazar BR, Serody JS. Leukocyte migration and graft-versus-host disease. Blood 2005;105:4191–9.
32. Martin PJ, Rizzo JD, Wingard JR, Ballen K, Curtin PT, Cutler C, et al. First- and second-line systemic treatment of acute graft-versus-host disease: recommendations of the American Society of Blood and Marrow Transplantation. Biol Blood Marrow Transplant 2012;18:1150–63.
33. Ok CY, Chen J, Xu-Monette ZY, Tzankov A, Manyam GC, Li L, et al. Clinical implications of phosphorylated STAT3 expression in *de novo* diffuse large B-cell lymphoma. Clin Cancer Res 2014;20:5113–23
34. Malynn BA, Ma A. A20 takes on tumors: tumor suppression by an ubiquitin-editing enzyme. J Exp Med 2009;206:977–80.
35. Choi J, Cooper ML, Alahmari B, Ritchey J, Collins L, Holt M, et al. Pharmacologic blockade of JAK1/JAK2 reduces GvHD and preserves the graft-versus-leukemia effect. PLoS ONE 2014;9:e109799.
36. Jung U, Foley JE, Erdmann AA, Eckhaus MA, Fowler DH. CD3/CD28 costimulated T1 and T2 subsets: differential *in vivo* allosensitization generates distinct GVT and GVHD effects. Blood 2003;102:3439–46.
37. Muranski P, Borman ZA, Kerkar SP, Klebanoff CA, Ji Y, Sanchez-Perez L, et al. Th17 cells are long lived and retain a stem cell-like molecular signature. Immunity 2011;35:972–85.
38. Reddy P. Pathophysiology of acute graft-versus-host disease. Hematol Oncol 2003;21:149–61
39. Sato T, Thorlacius H, Johnston B, Staton TL, Xiang W, Littman DR, et al. Role for CXCR6 in recruitment of activated $CD8^+$ lymphocytes to inflamed liver. J Immunol 2005;174:277–83.
40. Murai M, Yoneyama H, Harada A, Yi Z, Vestergaard C, Guo B, et al. Active participation of CCR5(+)CD8(+) T lymphocytes in the pathogenesis of liver injury in graft-versus-host disease. J Clin Invest 1999; 104:49–57.